The Journal of Chemical Physics

State variables for glasses: The case of amorphous ice

Cite as: J. Chem. Phys. **150**, 224502 (2019); https://doi.org/10.1063/1.5092586
Submitted: 12 February 2019 . Accepted: 14 May 2019 . Published Online: 10 June 2019

Nicolas Giovambattista, Francis W. Starr, and Peter H. Poole

The Journal of Chemical Physics ARTICLE scitation.org/journal/jcp

State variables for glasses: The case of amorphous ice

Cite as: J. Chem. Phys. 150, 224502 (2019); doi: 10.1063/1.5092586
Submitted: 12 February 2019 • Accepted: 14 May 2019 •
Published Online: 10 June 2019

Nicolas Giovambattista,[1,2,a)] Francis W. Starr,[3] and Peter H. Poole[4]

AFFILIATIONS

[1]Department of Physics, Brooklyn College of the City University of New York, Brooklyn, New York 11210, USA
[2]Ph.D. Programs in Chemistry and Physics, The Graduate Center of the City University of New York, New York, New York 10016, USA
[3]Department of Physics, Wesleyan University, Middletown, Connecticut 06459, USA
[4]Department of Physics, St. Francis Xavier University, Antigonish, Nova Scotia B2G 2W5, Canada

Note: This paper is part of a JCP Special Topic on Chemical Physics of Supercooled Water.
[a)]**Electronic mail:** ngiovambattista@brooklyn.cuny.edu

ABSTRACT

Glasses are out-of-equilibrium systems whose state cannot be uniquely defined by the usual set of equilibrium state variables. Here, we seek to identify an expanded set of variables that uniquely define the state of a glass. The potential energy landscape (PEL) formalism is a useful approach within statistical mechanics to describe supercooled liquids and glasses. We use the PEL formalism and computer simulations to study the transformations between low-density amorphous ice (LDA) and high-density amorphous ice (HDA). We employ the ST2 water model, which exhibits an abrupt first-order-like phase transition from LDA to HDA, similar to that observed in experiments. We prepare a number of distinct samples of both LDA and HDA that have completely different preparation histories. We then study the evolution of these LDA and HDA samples during compression and decompression at temperatures sufficiently low that annealing is absent and also during heating. We find that the evolution of each glass sample, during compression/decompression or heating, is uniquely determined by six macroscopic properties of the initial glass sample. These six quantities consist of three conventional thermodynamic state variables, the number of molecules N, the system volume V, and the temperature T, as well as three properties of the PEL, the inherent structure (IS) energy E_{IS}, the IS pressure P_{IS}, and the average curvature of the PEL at the IS $\mathcal{S}_{IS}$. In other words, $(N, V, T, E_{IS}, P_{IS}, \mathcal{S}_{IS})$ are state variables that define the glass state in the case of amorphous ice. An interpretation of our results in terms of the PEL formalism is provided. Since the behavior of water in the glassy state is more complex than for most substances, our results suggest that these six state variables may be applicable to amorphous solids in general and that there may be situations in which fewer than six variables would be sufficient to define the state of a glass.

I. INTRODUCTION

Equilibrium systems can be characterized by a few macroscopic thermodynamic variables.[1] For example, the thermodynamic state of a one-component equilibrium liquid is uniquely defined by three state variables, such as (N, V, T) or (N, P, T). Here, N, T, V, and P are, respectively, the number of molecules in the system, the temperature, the volume, and the pressure. Consequently, if two samples of the same liquid at equilibrium have the same state variables, then they are macroscopically identical, meaning that they will exhibit the same thermodynamic response when subjected to a given process, such as isothermal compression or isobaric heating. The situation is very different in the case of glasses (amorphous solids). Glasses are out-of-equilibrium systems, and their response to a specific process may depend strongly on the history of the system during the preparation of the glass sample. For example, two glasses made of the same substance and found to have identical values of (N, V, T) may not necessarily exhibit the same behavior when subjected to isothermal compression. It is apparent that the difficulty in predicting the behavior of glasses originates, at least partially, in our inability to properly characterize the glass state. Equilibrium state variables such as (N, V, T) need, somehow, to be complemented with additional variables to define the state of a glass. But how many state variables are required to characterize the glass state? How do we identify

these new variables? These are fundamental questions that need to be answered in order to extend equilibrium thermodynamics to the description of glasses. In this work, we address these questions for the case of a one-component system, water. Water is a particularly interesting test case due to its ubiquity and importance, as well as the complexity of the glassy states of water. To make progress on these questions, we apply concepts from the potential energy landscape (PEL) formalism.[2]

For a system of N atoms, the PEL is the hypersurface in $(3N + 1)$-dimensional space defined by the potential energy of the system as a function of the atomic coordinates, $\mathcal{V}(\vec{r}_1, \vec{r}_2, \ldots, \vec{r}_N)$.[3] At any given time t, the system is represented by a single point on the PEL given by the atomic coordinates at t. Hence, as the atomic coordinates change with time, the representative point of the system moves, describing a trajectory on the PEL. In the liquid state at high T, the system explores large regions of the PEL, while at low T the representative point is constrained to move within more localized regions of the PEL. Upon further cooling to the glass state, ergodicity is broken and the representative point of the system can only move within specific basins of the PEL. The local minimum of a PEL basin is called an inherent structure (IS). A complete theory for low-T liquids based on the topography of the PEL has been developed. This theory allows the free energy of the liquid to be formally expressed in terms of the IS energy E_{IS} (basin depth), the Hessian of the PEL at the IS (basin curvature), and the distribution of IS energies in the PEL (density of IS states).[4] For example, the PEL approach has recently been applied to the case of TIP4P/2005 water to obtain the $P(V, T)$ equation of state.[5]

The PEL has also been used to study out-of-equilibrium liquids and glasses. It has been shown that for glasses and out-of-equilibrium liquids cooled at a sufficiently slow rate at constant volume, the system can be described by a single parameter (E_{IS}), in that the behavior of the system during the cooling process can be quantified in terms of the properties of the equilibrium liquid at the same E_{IS}.[6] Unfortunately, this approach fails for liquids cooled more rapidly.[6–8] An extension of the approach of Ref. 6 to the case of glasses subjected to compression/decompression processes is not possible either because the IS sampled by the glass during these processes is different from the IS sampled by the equilibrium liquid.[8–10]

Here, we explore the possibility that state variables for the glass state can be identified among the quantities that arise in the PEL formalism. As indicated above, previous work using the PEL approach has demonstrated the importance of E_{IS}. Also important are the IS pressure P_{IS} and the shape function $\mathcal{S}_{IS}$ which quantifies the average curvature at the minima of the IS basins. Detailed definitions of E_{IS}, P_{IS}, and $\mathcal{S}_{IS}$ are given in Ref. 4. In the present work, we perform out-of-equilibrium molecular dynamics (MD) simulations of glassy water and show that when the traditional state variables (N, V, T) are augmented by $(E_{IS}, P_{IS}, \mathcal{S}_{IS})$, these six quantities together are a sufficient set of variables to characterize the glass state. That is, regardless of how differently two samples of glassy water are prepared, if they share the same values of $(N, V, T, E_{IS}, P_{IS}, \mathcal{S}_{IS})$, then the two samples will behave identically when subjected to processes such as compression, decompression, or heating. Unexpectedly, we further show that V cannot be interchanged with P as a state variable for these amorphous states.

Our choice of glassy water as the model system for the present study is based on the complex behavior that water exhibits in the glass state (see, e.g., Refs. 11–14). Experimentally, water can exist in at least two glass states, low-density amorphous ice (LDA) and high-density-amorphous ice (HDA).[15–17] LDA can be prepared, for example, by hyperquenching the liquid below $T \approx 130$ K at normal pressure.[18] Rapidly cooling liquid water at high pressure leads to HDA.[19] Remarkably, LDA and HDA can be interconverted by isothermal compression and decompression in the T range 130–140 K. The LDA-HDA transformation is extremely sharp and involves large changes in the properties of glassy water. For example, the density increases by more than 20% during the compression-induced LDA-to-HDA transformation.[15] The sharp changes observed during the LDA/HDA transformation are consistent with the interpretation that it is a first-order phase transition between two out-of-equilibrium states.[11,15,20] Such a picture is supported by the liquid-liquid phase transition (LLPT) hypothesis, which was proposed to explain the unusual behavior of liquid water at low T.[11] The LLPT hypothesis originated from MD simulations of ST2 water[21] which were recently confirmed by free energy calculations (see Ref. 22 and the references therein). Computer simulations of glassy water are also consistent with the LLPT hypothesis.[23–29] Recent experiments[30] and combined theoretical/computational studies[5,31] strongly support the possibility that water exists in two different liquid states at low temperatures.[32–34]

Our approach to characterize the glass state, based on concepts from the PEL formalism, differs from other approaches that have been pursued in recent years. One natural approach to identify the state of a glass has been to search for order parameters that characterize the local and/or intermediate-range structure of the material. A multitude of such order parameters have been proposed to characterize the local structure of liquids and glasses, for both atomic (see, e.g., Refs. 35–39) and molecular systems, including water (see, e.g., Refs. 29 and 40–42). However, it is not evident how many and what order parameters are appropriate to differentiate the states of a glassy material. Order parameters that do a good job in characterizing the glass state of a given substance may fail in the case of another. In addition, it is challenging to measure order parameter metrics in many experiments since they often require access to atomic coordinates. Our hope is that the general nature of the PEL will make the order parameters we consider here more generally applicable.

Another type of approach to describe glasses focuses on establishing a one-to-one correspondence between the glass state and the equilibrium liquid. These approaches are based on the concept of "fictive" temperature T_f and include the well-known Tool-Narayanaswamy (TN) formalism.[43–45] The TN approach has been successfully used to predict the behavior of polymers in the out-of-equilibrium liquid and glassy states.[46–50] Unfortunately, the TN formalism is based on empirical parameters that need to be extracted from experiments and on a few *Ansätze* that do not always apply.[44,46,47,50–52] In general, it is unclear whether glasses, when subjected to arbitrary processes, can be related to the equilibrium liquid state via a single-parameter fictive temperature. Indeed, computer simulations of glasses obtained by fast-cooling of the liquid[8,53] and glasses subject to isothermal compression/decompression[8–10,54,55] show that the IS sampled by the glass are never explored by the equilibrium liquid. We also note other theoretical approaches that have been developed to describe the behavior of glasses. Some of these approaches involve novel but abstract concepts, such as

space-time trajectories accessible to the glass state; see, e.g., Ref. 56 and the references therein.

This work is organized as follows. In Sec. II, we describe our computer simulation methods. The results are presented in Sec. III, which consists of a series of comparative studies of independently generated glassy water samples. In each case, we find that the set of variables $(N, V, T, E_{IS}, P_{IS}, \mathcal{S}_{IS})$ unambiguously characterizes the glass and determines its response to changes in P or T. A summary and discussion is included in Sec. IV. We provide additional examples to support our conclusions in the supplementary material.

II. MOLECULAR SIMULATION DETAILS

We perform out-of-equilibrium molecular dynamics (MD) simulations of a system composed of $N = 1728$ water molecules in a cubic box with periodic boundary conditions. Water molecules are represented using the ST2 model[57] with the long-range electrostatic interactions treated using the reaction field technique.[58] We use the reaction field approach rather than more sophisticated Ewald methods for consistency with the historic implementation of this model; in particular, Refs. 25 and 59 provide valuable reference data sets for the ST2 system. In all simulations, T and P are controlled using a Berendsen thermostat and barostat, respectively. To implement cooling/heating runs, we change the thermostat temperature linearly with time, with a cooling/heating rate of magnitude $q_T = dT/dt = 30$ K/ns. Similarly, to conduct compression/decompression runs, the barostat pressure changes linearly at a constant rate of magnitude $q_P = dP/dt = 300$ MPa/ns; see Ref. 25 for details. For each heating, compression, or decompression study, we generate 10 independent starting configurations using the same protocol for sample preparation. These 10 configurations are then each subjected to the chosen process (e.g., heating or compression) to allow us to assess the effect of sample-to-sample variations in the starting configurations. We note that recent work has shown that the Berendsen barostat gives correct results for static thermodynamic properties such as the pressure and density but does not correctly model properties that depend on fluctuations of the pressure.[60] Accordingly, we report here only on observables that do not depend on system fluctuations. Furthermore, thermodynamic quantities, such as the density of the amorphous ices across the LDA-HDA transformations, are not sensitive to the specific barostat employed.[27,28]

In order to calculate the PEL properties sampled by the system, we save configurations every 10 MPa during the compression/decompression runs and every 10 K during the heating runs. The procedure to evaluate the PEL properties of our system is identical to that followed in our previous works,[10,61] to which we refer the reader for details. For each configuration, the structure of the system at the IS (i.e., nearest local minimum of the PEL) is obtained using the conjugate gradient algorithm.[62] The energy of the system at this local minimum is the IS energy E_{IS}. The virial expression for the pressure at the IS configuration defines the IS pressure P_{IS}. The curvature of the PEL at the IS is quantified by the shape function $\mathcal{S}_{IS}$, which is directly linked to the vibrational density of states.

We compare the response of samples of LDA formed by different preparation protocols. Three forms of LDA are considered, labeled here as LDA-c, LDA-i, and LDA-d. These LDA forms were defined and studied in previous work[10,25,26,61] wherein full details may be found. Briefly, these systems are obtained as follows:

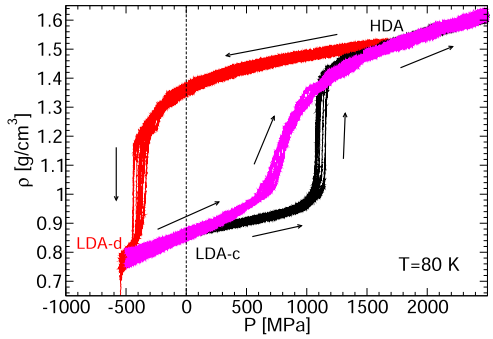

FIG. 1. ρ as a function of P during the compression of LDA-c formed at $P = 0.1$ MPa (black lines). At $P = 1100$–1200 MPa, LDA-c transforms to HDA. Decompression of HDA from $P = 1700$ MPa (red lines) results in LDA-d at $P \simeq -500$ MPa, and further decompression of LDA-d leads to the fracture of the amorphous ice at $P < -550$ MPa. Magenta lines correspond to the recompression of LDA-d back to HDA. At $P = 0.1$ MPa and $\rho \simeq 0.86$ g/cm^3, LDA-c and LDA-d have the same (N, V, T, P) and yet their behavior during compression at $P > 0.1$ MPa is remarkably different (black and magenta lines). In all cases, $T = 80$ K and the compression/decompression rate is $q_P = 300$ MPa/ns.

1. **LDA-c** is prepared by cooling the equilibrium liquid from $T = 350$ K to $T = 80$ K at constant $P = 0.1$ MPa and cooling rate $q_T = 30$ K/ns.
2. **LDA-i** is prepared from liquid configurations equilibrated at $P = 0.1$ MPa and at various starting temperatures $T_0 = 255, 260, 265, \ldots, 290$, and 300 K. After equilibration, these liquid configurations are cooled instantaneously to $T = 80$ K by rescaling the velocities of the atoms. That is, LDA-i is obtained with an infinite cooling rate. As a consequence, the starting LDA-i samples have the same density and are structurally identical to the equilibrium liquid at the starting temperature T_0.
3. **LDA-d** is prepared by a somewhat more complicated recipe, which is illustrated in Fig. 1. Specifically, LDA-d is prepared by first compressing LDA-c at $T = 80$ K from $P = 0.1$ MPa to $P = 1700$ MPa; see the black lines in Fig. 1, which show the density ρ as a function of P during compression. The sharp increase in ρ at $P \simeq 1150$ MPa corresponds to the transformation of LDA-c to HDA. The HDA form so produced is then decompressed at $T = 80$ K back to the LDA state at $P = -500$ MPa;[10,25] see the red lines in Fig. 1. It is this LDA form recovered at $P = -500$ MPa that we refer to as LDA-d.

To prepare three samples of HDA with different preparation histories, we compress LDA-c, LDA-i (with T_0 in the range 255–300 K), and LDA-d to $P = 1700$ MPa at $T = 80$ K.

III. RESULTS

A. Standard thermodynamic variables are not sufficient to characterize the glass state

In this section, we provide an example from our simulations of glassy water that shows that neither the set of thermodynamic

variables (N, V, T) nor the expanded set (N, V, T, P) are sufficient to identify the glass state. To do so, we subject both LDA-c and LDA-d to isothermal compression at T = 80 K. Figure 1 shows ρ for LDA-c during compression (black lines) starting from P = 0.1 MPa, where the sharp transition to HDA is observed near 1150 MPa, as noted in Sec. II. The magenta lines in Fig. 1 show ρ for LDA-d during compression. We observe that LDA-d undergoes a much more gradual density change than LDA-c over a range of P from 700 to 1100 MPa as it transforms to HDA.

Note that in Fig. 1 the LDA-c and LDA-d compression curves pass through the same point, located at $P \simeq 0.1$ MPa and $\rho \simeq 0.86$ g/cm^3. At this point, both glasses exhibit the same values of the thermodynamic variables (N, V, T, P). However, the behavior of LDA-c and LDA-d during the subsequent compression for $P > 0.1$ MPa differs significantly (black and magenta lines). That is, despite sharing the same values of (N, V, T, P) at a particular point, the difference between these two glasses at this point, due to their different preparation histories, is revealed by their different responses to the subsequent compression. This is a clear example that neither (N, V, T) nor the expanded set (N, V, T, P) are a complete set of state variables for identifying the glassy state of water.

We note that experiments also show differences in the properties of LDA, depending on the preparation history. Specifically, the glass transition temperature of so-called LDA$_I$ and LDA$_{II}$, two subfamilies of LDA, differs slightly when they are heated at P = 0.1 MPa from T = 80 K.[63,64] In addition, during compression, the LDA-to-HDA transformation is smoother and occurs at slightly lower pressure for LDA$_I$ than for LDA$_{II}$.[64] Small differences in the properties of LDA are also observable when one considers other forms of LDA, such as ASW (amorphous solid water) and HGW (hyperquenched glassy water).[12]

B. State variables for glasses

In order to differentiate LDA-c from LDA-d, we examine the utility of generic variables obtained from the PEL. Figure 2 shows $E_{IS}(\rho)$, $P_{IS}(\rho)$, and $\mathcal{S}_{IS}(\rho)$ during the isothermal compression of LDA-c and LDA-d at T = 80 K. Notably, at $\rho \simeq 0.86$ g/cm^3, LDA-c and LDA-d share the same value of P_{IS} but exhibit very different values of E_{IS} and $\mathcal{S}_{IS}$. Figure 2 thus reveals that LDA-c and LDA-d, despite having the same values of (N, V, T, P) when $\rho \simeq 0.86$ g/cm^3, do not occupy the same region of the PEL under these conditions. That is, we find that thermodynamic PEL properties are able to expose the difference between these two glasses at $\rho \simeq 0.86$ g/cm^3.

Furthermore, we observe in Fig. 1 that LDA-c and LDA-d follow the same $\rho(P)$ curve when they have both entered the HDA regime at $P > 1500$ MPa and $\rho > 1.46$ g/cm^3. In Fig. 2, we find that for $\rho > 1.46$ g/cm^3, the curves for $E_{IS}(\rho)$, $P_{IS}(\rho)$, and $\mathcal{S}_{IS}(\rho)$ overlap for highly compressed LDA-d and LDA-c. This suggests that once LDA-d and LDA-c attain the same values of $(N, V, T, E_{IS}, P_{IS}, \mathcal{S}_{IS})$, then the behavior of these glasses during further compression, as quantified by $\rho(P)$, becomes indistinguishable. In other words, at least in this case, the variables $(N, V, T, E_{IS}, P_{IS}, \mathcal{S}_{IS})$ play the role of state variables for glassy water.

In the rest of this section as well as in the supplementary material, we test the generality of this conclusion by comparing the behavior of distinct amorphous ices when subjected to various processes. Specifically, we compare the behavior of different

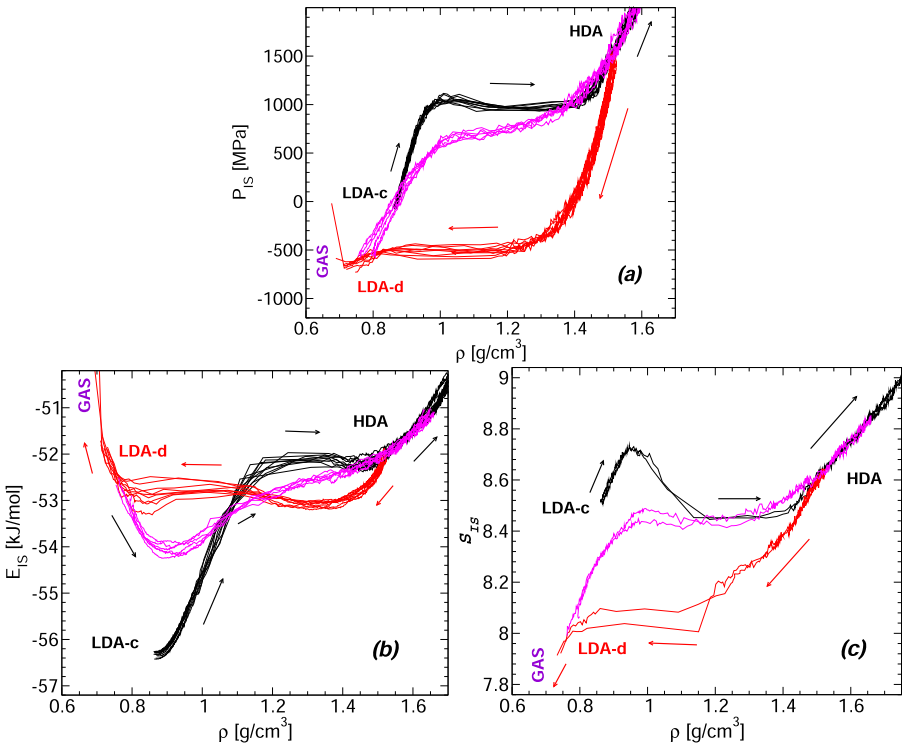

FIG. 2. (a) P_{IS}, (b) E_{IS}, and (c) $\mathcal{S}_{IS}$ at the IS sampled by the system during the compression and decompression processes shown in Fig. 1. Data are shown with the same colors used in Fig. 1. At $\rho \simeq 0.86$ g/cm^3, LDA-c and LDA-d have the same (N, V, T, P), but their PEL properties are not all identical (black and magenta lines).

LDA and HDA samples when subjected to isothermal compression (Sec. III B 1), isothermal decompression (Sec. III B 2), isochoric heating (Sec. III B 3), and isobaric heating (Sec. III B 4). In all cases, we find that the variables $(N, V, T, E_{IS}, P_{IS}, \mathcal{S}_{IS})$ fully describe the state of the glass.

1. Isothermal compression

We focus on the behavior of LDA-c, LDA-d, and LDA-i during compression at T = 80 K. Figure 3(a) shows $\rho(P)$ during the compression of LDA-c and LDA-d as well as LDA-i obtained from the liquid equilibrated at selected temperatures T_0. The corresponding behavior of $E_{IS}(\rho)$, $P_{IS}(\rho)$, and $\mathcal{S}_{IS}(\rho)$ is shown in Figs. 3(b)–3(d).

We discuss first the case of LDA-c and LDA-i. We see in Figs. 3(a)–3(d) that, at the starting pressure P = 0.1 MPa, LDA-c (black lines) and LDA-i (T_0 = 260 K) (brown lines) share the same values of $(N, V, T, E_{IS}, P_{IS}, \mathcal{S}_{IS})$. Therefore, according to our hypothesis, these two LDA forms should exhibit the same thermodynamic behavior, as indicated by $\rho(P)$, during compression at $P > 0.1$ MPa. Indeed, Fig. 3(a) shows that at all pressures studied ($0.1 \le P \le 1700$ MPa) the densities of LDA-c and LDA-i (T_0 = 260 K) are identical. In addition, both LDA forms also share the same values of E_{IS}, P_{IS}, and $\mathcal{S}_{IS}$, showing that they explore the same regions of the PEL and hence that they are the same amorphous ice.

The case of LDA-d and LDA-i is more subtle. At first glance, the density of LDA-d for $P > 0.1$ MPa lies very close to the $\rho(P)$ curves for LDA-i obtained from the liquid in the range T_0 = 280–300 K. However, a closer look at Fig. 3(a) indicates that the density of LDA-d (magenta lines) overlaps best with the density of LDA-i (T_0 = 290 K) (violet lines) and that this overlap sets in only for $P > 700$ K. We also note that at P = 700 MPa these two LDA forms have the same density ($\rho \simeq 1.0$ g/cm^3) and share the same values of $(N, V, T, E_{IS}, P_{IS}, \mathcal{S}_{IS})$. Therefore, according to our hypothesis, these two LDA forms should behave identically during compression only for $700 \le P \le 1700$ MPa. Indeed, Figs. 3(a)–3(d) shows that LDA-d and LDA-i (T = 290 K) have the same $\rho(P)$ curve and PEL properties $(E_{IS}(\rho), P_{IS}(\rho), \mathcal{S}_{IS}(\rho))$ for $700 < P \le 1700$ MPa.

2. Isothermal decompression

We next conduct a test similar to that discussed above but for the case of an isothermal decompression process. Specifically, we decompress LDA-c and several of the LDA-i forms obtained at P = 0.1 MPa from the equilibrium liquid over the range T_0 = 255–265 K. As discussed above, and shown in Figs. 4(a)–4(d), at P = 0.1 MPa and T = 80 K, LDA-c (blue lines) and LDA-i (T_0 = 260 K) (brown lines) exhibit the same values of $(N, V, T, E_{IS}, P_{IS}, \mathcal{S}_{IS})$. According to our hypothesis, we thus expect that these two LDA forms will follow the same $\rho(P)$ curve during the decompression process. The LDA-i forms for T_0 = 255 and 265 K both differ from LDA-c in terms of their E_{IS} and $\mathcal{S}_{IS}$ values at P = 0.1 MPa, and so we expect that these samples will not follow the same $\rho(P)$ curve as LDA-c during decompression. All of these predictions are confirmed in Fig. 4(a). In addition, and as expected, LDA-c and LDA-i (T_0 = 260 K) also maintain the same PEL properties $E_{IS}(\rho)$, $P_{IS}(\rho)$, and $\mathcal{S}_{IS}(\rho)$ during decompression.

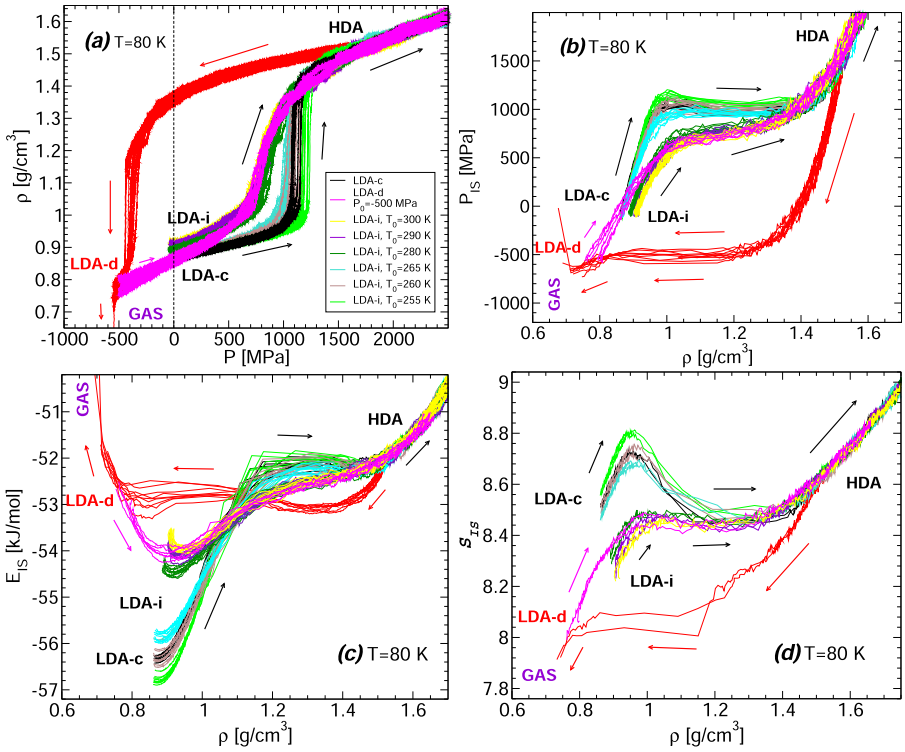

FIG. 3. (a) ρ as function of P during the compression of LDA-i formed at P = 0.1 MPa from liquids equilibrated at selected values of T_0. For comparison, we include the compression of LDA-d obtained at P = −500 MPa (magenta lines). Black and red lines indicate, respectively, the compression of LDA-c and subsequent decompression from P = 1700 MPa (HDA). The corresponding variations of P_{IS}, E_{IS}, and $\mathcal{S}_{IS}$ with ρ are shown in (b), (c), and (d). At P = 0.1 MPa and $\rho \simeq 0.86$ g/cm^3, LDA-c (black) and LDA-i (T_0 = 260 K) (brown) are characterized by the same $(N, V, T, E_{IS}, P_{IS}, \mathcal{S}_{IS})$; they also exhibit approximately the same $\rho(P)$ and PEL properties at $P > 0.1$ MPa. Similarly, at P = 700 MPa and $\rho \simeq 1.00$ g/cm^3, LDA-d (magenta) and LDA-i (T_0 = 290 K) (violet) are characterized by the same $(N, V, T, E_{IS}, P_{IS}, \mathcal{S}_{IS})$; they also exhibit approximately the same $\rho(P)$ and PEL properties at $P > 700$ MPa. In all cases, T = 80 K and the compression/decompression rate is q_P = 300 MPa/ns.

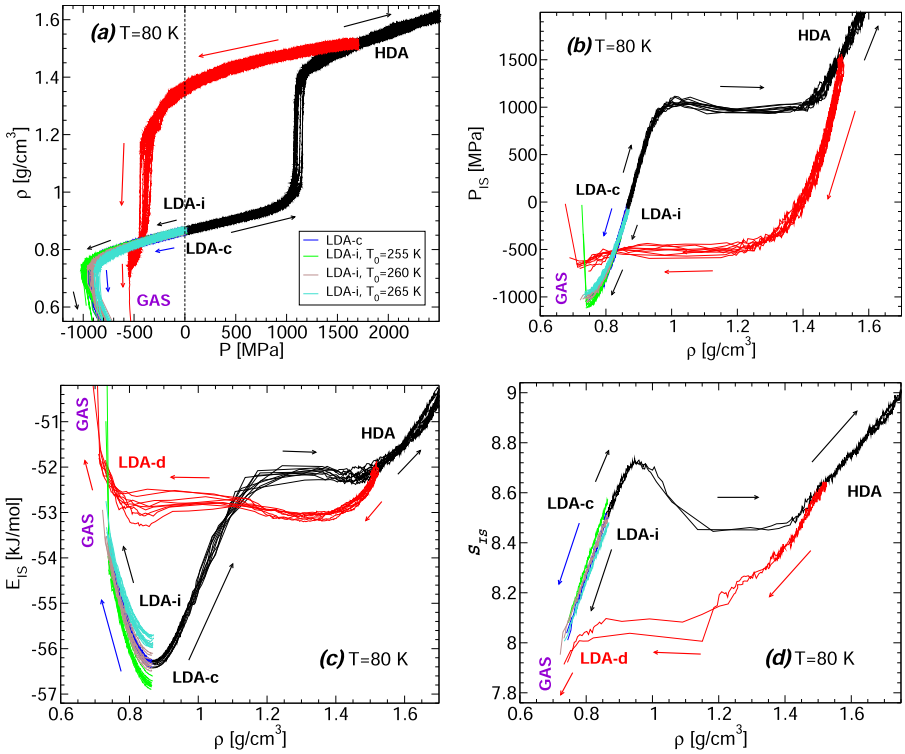

FIG. 4. (a) ρ as a function of P during the decompression of LDA-i formed at P = 0.1 MPa from liquids equilibrated at selected values of T_0. Black, red, and blue lines indicate, respectively, the compression of LDA-c, subsequent decompression from P = 1700 MPa (HDA), and decompression of LDA-c to negative pressures. Note that the blue lines coincide with, and so are almost totally covered by, the brown lines. The corresponding variations of P_{IS}, E_{IS}, and $\mathcal{S}_{IS}$ with ρ are shown in (b), (c), and (d). At P = 0.1 MPa and $\rho \simeq 0.86$ g/cm^3, LDA-c (blue and black) and LDA-i (T_0 = 260 K) (brown) are characterized by the same $(N, V, T, E_{IS}, P_{IS}, \mathcal{S}_{IS})$; they exhibit approximately the same $\rho(P)$ at $P < 0.1$ MPa. In all cases, T = 80 K and the compression/decompression rate is q_P = 300 MPa/ns.

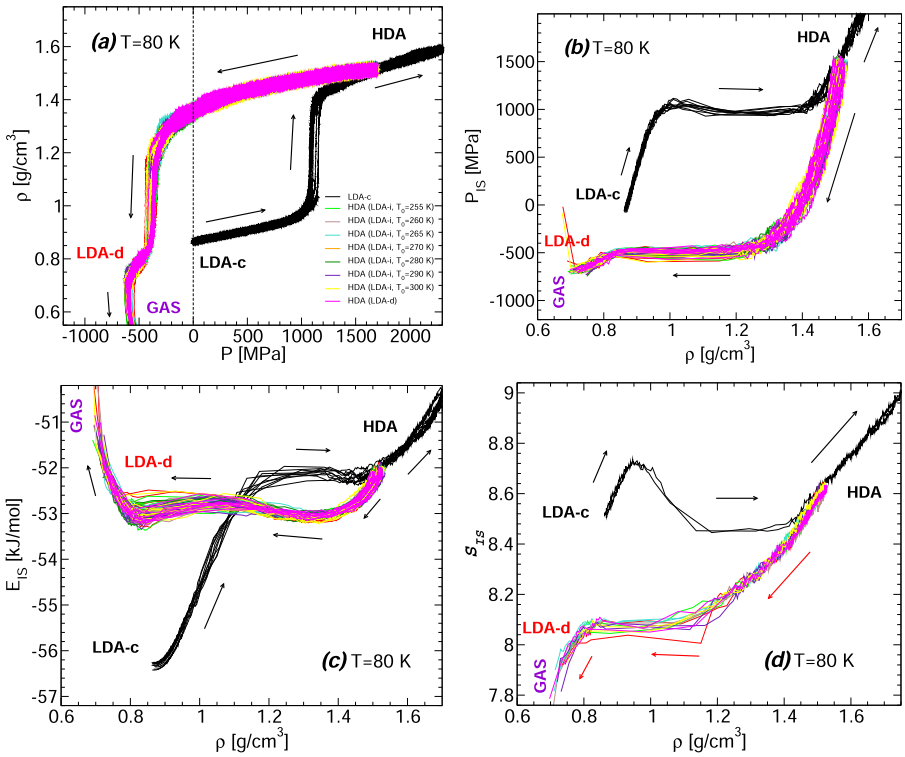

FIG. 5. (a) ρ as a function of P during decompression of HDA from P = 1700 MPa to negative pressures. HDA is prepared by compression of (i) LDA-c, (ii) LDA-i formed at P = 0.1 MPa from the liquid equilibrated at selected values of T_0, and (iii) LDA-d obtained at P_0 = −500 MPa. Black and red lines indicate, respectively, the compression of LDA-c leading to HDA and the subsequent decompression of HDA from P = 1700 MPa (from Fig. 3). The corresponding variations of P_{IS}, E_{IS}, and $\mathcal{S}_{IS}$ with ρ are shown in (b), (c), and (d). At P = 1700 MPa and $\rho \simeq 1.50$ g/cm^3, all HDA forms are characterized by the same $(N, V, T, E_{IS}, P_{IS}, \mathcal{S}_{IS})$; they exhibit approximately the same $\rho(P)$ and PEL properties at $P < 1700$ MPa until they fracture at $P \approx -550$ MPa. In all cases, T = 80 K and the compression/decompression rate is q_P = 300 MPa/ns.

A similar situation occurs when we decompress HDA samples obtained via different preparation histories. Here, we consider several HDA forms obtained by starting with LDA-c and all the LDA-i samples obtained for T_0 = 255–300 K, and compressing each from P = 0.1 MPa to 1700 MPa. A third HDA form is obtained by compressing LDA-d from P = −500 MPa to P = 1700 MPa. Figures 5(a)–5(d) show that all of the HDA forms so produced are identical at P = 1700 MPa, meaning that they are characterized by the same values of $(N, V, T, E_{IS}, P_{IS}, \mathcal{S}_{IS})$. During decompression at P < 1700 MPa, we therefore expect that all these HDA forms should exhibit the same thermodynamic behavior, as indicated by $\rho(P)$, and PEL properties $E_{IS}(\rho)$, $P_{IS}(\rho)$, and $\mathcal{S}_{IS}(\rho)$. This expectation is confirmed in Figs. 5(a)–5(d).

3. Isochoric heating

Next, we test whether LDA forms prepared in different ways, but having the same values of $(N, V, T, E_{IS}, P_{IS}, \mathcal{S}_{IS})$, behave identically upon heating at constant density ρ = 0.9 g/cm^3. All of our heating runs start from T = 80 K. We focus on LDA-c, LDA-d, and LDA-i; see Fig. 6. The LDA-c and LDA-i forms considered here are obtained at P = 0.1 MPa and T = 80 K, as explained in Sec. II. The density of LDA-c at these conditions is less than 0.90 g/cm^3, and so, we compress this LDA form at T = 80 K until it reaches ρ = 0.90 g/cm^3. Similarly, LDA-d is compressed from P = −500 MPa [where $\rho \simeq$ 0.75–0.80 g/cm^3, see Fig. 3(a)] until it reaches ρ = 0.90 g/cm^3. As shown in Fig. 6(a), the pressure of these LDA forms at ρ = 0.90 g/cm^3 differs by as much as 500 MPa, depending on the glass history. Even within the ten independent simulations of the LDA-d family, the pressure of the starting configurations differs by ∼300 MPa. For comparison, we also heat HDA decompressed from P = 1700 MPa down to P = −400 MPa so that the density of the resulting glass (which we call LDA-x) is ρ = 0.9 g/cm^3. The density of HDA during the decompression path, as it transforms to LDA-x, is indicated by the red lines in Fig. 3(a).

All of the starting configurations used for these heating runs have the same value of ρ and T and therefore have the same values of (N, V, T). During the heating runs at ρ = 0.90 g/cm^3, the only thermodynamic variable free to change is P. Accordingly, in Fig. 6(a), we include the evolution of $P(T)$ for all LDA forms considered. The responses of the PEL properties to heating, $E_{IS}(T)$, $P_{IS}(T)$, and $\mathcal{S}_{IS}(T)$, are shown in Figs. 6(b)–6(d).

We discuss first the case of LDA-c (black lines) and LDA-i (T_0 = 260 K) (brown lines). At T = 80 K, these LDA forms have identical values of $(N, V, T, E_{IS}, P_{IS}, \mathcal{S}_{IS})$. If they are in the same glass state, then we would expect LDA-c and LDA-i (T_0 = 260 K) to follow the same $P(T)$ curve during heating. Figure 6(a) shows that, within the distribution of pressures among the independent runs, the $P(T)$ curves of LDA-c and LDA-i (T_0 = 260 K) are in good agreement with each other for T > 80 K. In addition, LDA-c and LDA-i (T_0 = 260 K) exhibit similar PEL properties at T > 80 K.

Regarding LDA-d and LDA-i, we find that the PEL properties $(E_{IS}, P_{IS}, \mathcal{S}_{IS})$ differ for the starting configurations of LDA-d and LDA-i for all choices of T_0, as shown in Fig. 6. In other words, these LDA forms do not correspond to the same glass state at T = 80 K, and consistent with this, P is not the same either. However, starting at $T \simeq$ 200 K, we observe that the values of $(E_{IS}, P_{IS}, \mathcal{S}_{IS})$ for LDA-d (magenta lines) and LDA-i (T_0 = 280–300 K) (green, violet, and yellow lines) merge together. In other words, for T > 200 K, all of these LDA forms have the same $(N, V, T, E_{IS}, P_{IS}, \mathcal{S}_{IS})$, and hence, they should correspond to the same amorphous ice. In agreement with this view, Fig. 6(a) shows that all of these LDA forms exhibit the same $P(T)$ upon heating at T > 200 K.

We note that the same conclusion applies when comparing LDA-d (magenta lines) and LDA-x (maroon lines). These two amorphous ices share identical $(N, V, T, E_{IS}, P_{IS}, \mathcal{S}_{IS})$ at $T \simeq$ 190 K, and

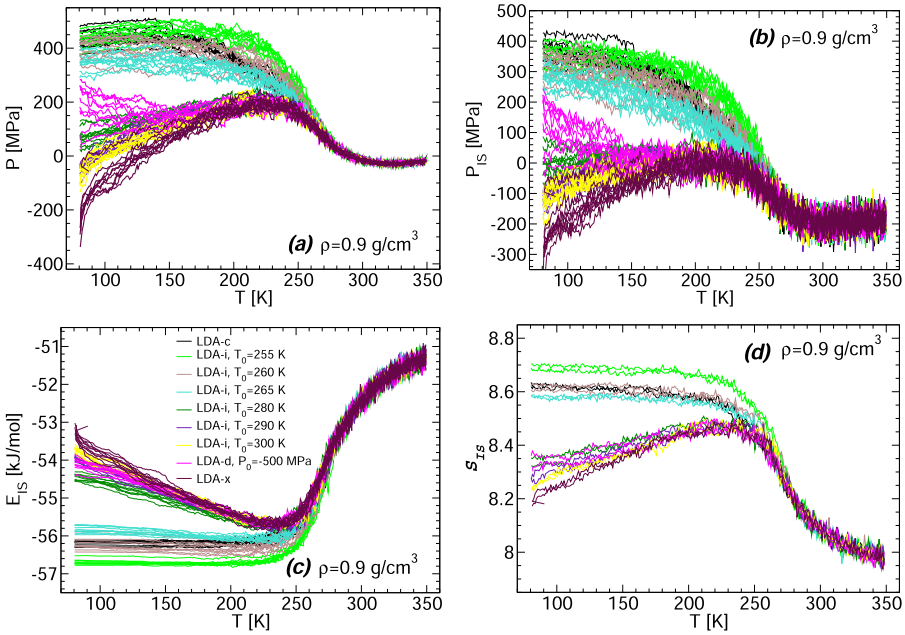

FIG. 6. (a) P as a function of T during isochoric heating at ρ = 0.9 g/cm^3 of LDA-c, LDA-i (formed at P = 0.1 MPa for different values of T_0), and LDA-d (formed at P_0 = −500 MPa). All these LDA forms are compressed at T = 80 K until they reach the density of 0.9 g/cm^3. Also included is the isobaric heating of LDA-x which is obtained by decompressing HDA until the density of 0.90 g/cm^3 is reached. The corresponding variations with T of P_{IS} (b), E_{IS} (c), and $\mathcal{S}_{IS}$ (d) are also shown. The heating rate is q_T = 30 K/ns.

accordingly, they exhibit the same $P(T)$ and PEL properties at higher T. We note that although LDA-d and LDA-x are both obtained by decompression of HDA, LDA-d is subjected to an additional compression starting from $P = -500$ MPa in order to obtain a sample with $\rho = 0.9$ g/cm^3. In other words, LDA-d and LDA-x are different glasses at $T = 80$ K.

We stress that the temperature $T = 200$ K at which LDA-c, LDA-i ($T_0 = 290$ K), and LDA-x reach the same glass state is *below* the temperature at which ergodicity is restored. For example, the mode coupling temperature of ST2 water at $\rho = 0.9$ g/cm^3 is $T_{MCT} \approx 237$ K[65] and the lowest T accessible to equilibrium MD simulations over a simulation time window of the order of 100 ns ($N = 1728$) is $T \sim 255$ K.[59] Therefore, all three LDA forms reach the same glass state at temperatures below the calorimetric glass transition temperature in ST2 water, for which $T_g \sim 270$–280 K at the particular heating rate used here[24,26]).

4. Isobaric heating

In this section, we compare the behavior of LDA and HDA forms during heating at a constant pressure of $P = 0.1$ MPa starting from $T = 80$ K. Our aim in this section is to test whether amorphous ices with the same $(N, P, T, E_{IS}, P_{IS}, \mathcal{S}_{IS})$ correspond to the same glass state. That is, can P replace V in the list of state variables?

We focus on the LDA-c, LDA-d, and LDA-i forms considered above. For HDA, we consider the recovered HDA decompressed from $P = 1700$ MPa down to $P = 0.1$ MPa [see the red lines in Fig. 3(a)]. The density of the resulting glass (which we call HDA-x) is $\rho \simeq 1.34$–1.38 g/cm^3. We note that during the heating runs at $P = 0.1$ MPa the only thermodynamic variable free to change is ρ. Accordingly, in Fig. 7(a), we include the evolution of $\rho(T)$ for all amorphous ices considered. The corresponding PEL properties $E_{IS}(T)$, $P_{IS}(T)$, and $\mathcal{S}_{IS}(T)$ are shown in Figs. 7(b)–7(d).

Our first test compares LDA-c and LDA-i ($T_0 = 260$ K). In this case, both LDA forms (black and brown lines) share the same values of $(N, P, T, E_{IS}, P_{IS}, \mathcal{S}_{IS})$ at the starting state ($P = 0.1$ MPa, $T = 80$ K); see Figs. 7(a)–7(d). Moreover, both glasses have identical $\rho(T)$ and PEL properties at all temperatures during the heating process. Therefore, one might conclude that the variables $(N, P, T, E_{IS}, P_{IS}, \mathcal{S}_{IS})$ can also be used as state variables for our glasses. However, we note that at the starting state, LDA-c and LDA-i ($T_0 = 260$ K) have the same ρ. This means that, for this particular test, the starting LDA samples also share the same values of $(N, V, T, E_{IS}, P_{IS}, \mathcal{S}_{IS})$. Consequently, this example is not sufficient to discriminate between the use of P and V as a state variable for glasses.

We focus next on the behavior of LDA-d and LDA-i shown in Fig. 7. In the temperature range 80 K < T < 200 K, the PEL properties of LDA-d (magenta lines) coincide with LDA-i ($T_0 = 290$ K) (violet lines), and so, they share the same values of $(N, P, T, E_{IS}, P_{IS}, \mathcal{S}_{IS})$ in this T range. Yet Fig. 7(a) shows that $\rho(T)$ for LDA-d and LDA-i ($T_0 = 290$ K) differs by as much as 0.05 g/cm^3 in the same T range. This counterexample shows that the variables $(N, P, T, E_{IS}, P_{IS}, \mathcal{S}_{IS})$ do not work as state variables for amorphous ices.

A similar situation holds when comparing LDA-d (magenta lines) and HDA-x (maroon lines). LDA-d and HDA-x are very different at $T < 200$ K with a density difference of $\simeq 0.5$ g/cm^3 at $T = 80$ K. This is because HDA-x transforms to an LDA-like state only at $T \simeq 200$ K. The transformation of HDA-x to an LDA-like state is described in detail in Refs. 24 and 26 and can be identified by the decrease in density in Fig. 7(a) at $T \simeq 180$ K and the sudden changes in the PEL properties [Figs. 7(b)–7(d)] at $T \simeq 160$–200 K. In Figs. 7(b)–7(d), we see that at $T = 200$ K the PEL properties of both amorphous ices overlap with one another. However, at this same temperature, the $\rho(T)$ curve for LDA-d (magenta lines) remains different from that for HDA-x (maroon lines). Again, this shows that

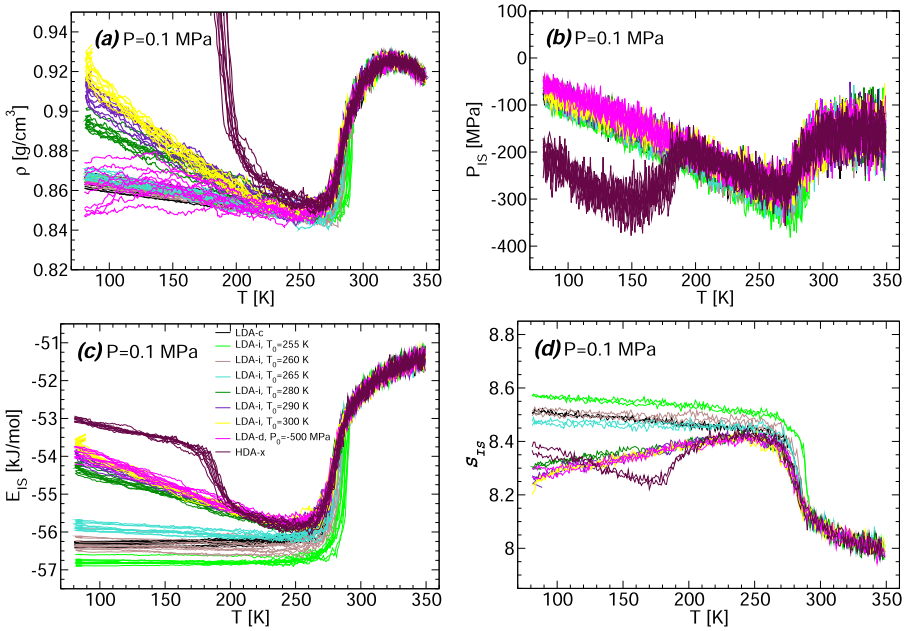

FIG. 7. (a) ρ as a function of T during isobaric heating at $P = 0.1$ MPa of LDA-c, LDA-i (formed at $P = 0.1$ MPa for different values of T_0), and LDA-d (formed at $P_0 = -500$ MPa and recompressed to $P = 0.1$ MPa). Also included is the isobaric heating of HDA-x which is obtained by decompressing HDA to $P = 0.1$ MPa. The corresponding variations with T of P_{IS} (b), E_{IS} (c), and $\mathcal{S}_{IS}$ (d) are also shown. In all panels, $P = 0.1$ MPa and the heating rate is $q_T = 30$ K/ns.

the variables $(N, P, T, E_{IS}, P_{IS}, \mathcal{S}_{IS})$ do not represent state variables for amorphous ices.

IV. SUMMARY AND DISCUSSION

In this work, we performed detailed computer simulations to study the behavior of amorphous ices with distinct preparation histories when subjected to various processes: isothermal compression and decompression, isochoric heating, and isobaric heating. Additional comparative studies of the behavior of independent amorphous ices are provided in the supplementary material, which include (a) HDA forms prepared at $P = 400$ MPa during isothermal compression/decompression at $T = 80$ K; (b) HDA forms prepared at $P = 1000$ MPa during isothermal compression/decompression at $T = 80$ K; (c) HDA forms prepared by compression of LDA and ice I_h, which are then subjected to isothermal decompression at $T = 80$ K; and (d) LDA forms prepared at $P = 0.1$ MPa during isothermal compression at $T = 180$ K. In all cases, we find that amorphous ices that have the same variables $(N, V, T, E_{IS}, P_{IS}, \mathcal{S}_{IS})$ behave identically upon compression, decompression, and heating. In other words, these six thermodynamic variables are a sufficient set of variables to characterize the glass state of water. We note that, in the thermodynamic limit $(N \to \infty)$, our results imply that one could also consider the reduced set of five variables $(\rho, T, e_{is} = E_{IS}/N, P_{IS}, \mathcal{S}_{IS})$ to identify the state of a glass. Interestingly, we also find that the alternative set of variables $(N, P, T, E_{IS}, P_{IS}, \mathcal{S}_{IS})$ cannot be used to characterize the glass state.

To understand why the variables $(N, V, T, E_{IS}, P_{IS}, \mathcal{S}_{IS})$ are state variables for glassy water, we note that two glasses with the same number of molecules N are characterized by the same PEL. Requiring that the two glasses also share the same volume V implies that both systems are constrained to explore the same region of the PEL. For example, in the case of a system of N atoms in a cubic box of volume $V = L^3$, all atomic coordinates are constrained to the range $[0, L]$. At the same T, both glasses have the same average kinetic energy to overcome potential energy barriers of the PEL. The question is then why should identical glasses also be characterized by same values of $(E_{IS}, P_{IS}, \mathcal{S}_{IS})$? While we do not offer a proof, this observation can be physically rationalized by interpreting $(E_{IS}, P_{IS}, \mathcal{S}_{IS})$ as variables that "label" the region of the PEL explored by the system. Two systems that explore the same region of the PEL must explore the same microstates and so will have the same values of $(E_{IS}, P_{IS}, \mathcal{S}_{IS})$.

For the same reason, we can understand why the variables $(N, P, T, E_{IS}, P_{IS}, \mathcal{S}_{IS})$ fail to characterize the glass state. Specifically, by fixing P and not V, we cannot be sure that two glasses are constrained to sample the same volume of the PEL. So even if the two glassy systems sample IS with identical values of $(E_{IS}, P_{IS}, \mathcal{S}_{IS})$, they may not necessarily explore the same basins of the PEL, and hence, the same microstates.

We emphasize that in this work we conclude that the set of variables $(N, V, T, E_{IS}, P_{IS}, \mathcal{S}_{IS})$ is a complete set of variables to characterize the glass state for the case of amorphous ice. However, it is possible that other substances may require fewer PEL variables to characterize the glass state. For example, it may be possible that the set $(N, V, T, E_{IS}, \mathcal{S}_{IS})$ is sufficient to identify the glass state of many simpler glass forming systems where strong directional bonds do not play a role. Similarly, one may need additional variables, other than $(N, V, T, E_{IS}, P_{IS}, \mathcal{S}_{IS})$, to characterize the glass state of multicomponent mixtures. The main point of our work is to show that it is possible to use a small number of variables obtained from the PEL, complemented by (N, V, T), to identify the region of the PEL (and hence the microstates) accessible to glasses and perhaps other out-of-equilibrium systems such as liquids subject to sudden changes in T or V. Moreover, we show that this set of six variables is sufficient for the practically important case of water.

Finally, we note that an important goal for future work is to identify observables accessible in experiments, corresponding to PEL variables such as $(P_{IS}, E_{IS}, \mathcal{S}_{IS})$. For example, $\mathcal{S}_{IS}$ can be evaluated from the vibrational density of states measured experimentally. Our work demonstrates that, at least for water, a small number of macroscopic properties are sufficient to unambiguously identify the glass state, without knowledge of its preparation history. As a consequence, experimental efforts to measure the PEL properties of glasses may provide a valuable practical tool for assessing the nature of a given glassy sample and predicting its response to mechanical and thermal stress relative to other samples.

SUPPLEMENTARY MATERIAL

See supplementary material for additional comparative studies of the behavior of independent amorphous ices under compression and decompression processes.

ACKNOWLEDGMENTS

We thank F. Sciortino for enlightening discussions. This project was supported, in part, by a grant of computer time from the City University of New York High Performance Computing Center under NSF Grant Nos. CNS-0855217, CNS-0958379, and ACI-1126113. P.H.P. thanks NSERC, ACENET, Compute Canada, and the Dr. W. F. James Research Chair Program. We thank Wesleyan University for computational resources. F.W.S. was supported by NIST Award No. 70NANB15H282.

REFERENCES

[1] H. B. Callen, *Thermodynamics and an Introduction to Thermostatistics* (John Wiley & Sons, Inc., New York, 1985).
[2] F. H. Stillinger, *Energy Landscapes, Inherent Structures, and Condensed-Matter Phenomena* (Princeton University Press, New Jersey, 2016).
[3] F. H. Stillinger, Science **267**, 1935 (1995).
[4] F. Sciortino, J. Stat. Mech.: Theory Exp. **2005**, P05015.
[5] P. H. Handle and F. Sciortino, J. Chem. Phys. **148**, 134505 (2018).
[6] W. Kob, F. Sciortino, and P. Tartaglia, Europhys. Lett. **49**, 590 (2000).
[7] F. Sciortino and P. Tartaglia, Phys. Rev. Lett. **86**, 107–110 (2000).
[8] S. Mossa, G. Ruocco, F. Sciortino, and P. Tartaglia, Philos. Mag. B **82**, 695–705 (2000).
[9] N. Giovambattista, H. E. Stanley, and F. Sciortino, Phys. Rev. Lett. **91**, 115504 (2003).
[10] N. Giovambattista, F. Sciortino, F. W. Starr, and P. H. Poole, J. Chem. Phys. **145**, 224501 (2016).
[11] O. Mishima and H. E. Stanley, Nature **396**, 329 (1998).
[12] P. G. Debenedetti, J. Phys.: Condens. Matter **15**, R1669 (2003).
[13] C. A. Angell, Annu. Rev. Phys. Chem. **55**, 559 (2004).
[14] T. Loerting and N. Giovambattista, J. Phys.: Condens. Matter **18**, R919 (2006).
[15] O. Mishima, J. Chem. Phys. **100**, 5910 (1994).
[16] O. Mishima, L. D. Calvert, and E. Whalley, Nature **310**, 393 (1984).

[17]O. Mishima, L. D. Calvert, and E. Whalley, Nature **314**, 76 (1985).
[18]E. Mayer, J. Appl. Phys. **58**, 663 (1985).
[19]O. Mishima and Y. Suzuki, J. Chem. Phys. **115**, 4199 (2001).
[20]K. Winkel, E. Mayer, and T. Loerting, J. Phys. Chem. B **115**, 14141 (2011).
[21]P. H. Poole, F. Sciortino, U. Essmann, and H. E. Stanley, Nature **360**, 324 (1992).
[22]J. C. Palmer, P. H. Poole, F. Sciortino, and P. G. Debenedetti, Chem. Rev. **118**, 9129 (2018).
[23]P. H. Poole, U. Essmann, F. Sciortino, and H. E. Stanley, Phys. Rev. E **48**, 4605 (1993).
[24]N. Giovambattista, T. Loerting, B. R. Lukanov, and F. W. Starr, Sci. Rep. **2**, 390 (2012).
[25]J. Chiu, F. W. Starr, and N. Giovambattista, J. Chem. Phys. **139**, 184504 (2013).
[26]J. Chiu, F. W. Starr, and N. Giovambattista, J. Chem. Phys. **140**, 114504 (2013).
[27]J. Wong, D. A. Jahn, and N. Giovambattista, J. Chem. Phys. **143**, 074501 (2015).
[28]J. Engstler and N. Giovambattista, J. Chem. Phys. **147**, 074505 (2017).
[29]F. Martelli, N. Giovambattista, S. Torquato, and R. Car, Phys. Rev. Mater. **2**, 075601 (2018).
[30]K. H. Kim *et al.*, Science **358**, 1589 (2017).
[31]J. W. Biddle *et al.*, J. Chem. Phys. **146**, 034502 (2017).
[32]P. Gallo *et al.*, Chem. Rev. **116**, 7463 (2016).
[33]N. J. Hestand and J. L. Skinner, J. Chem. Phys. **149**, 140901 (2018).
[34]P. H. Handle, T. Loerting, and F. Sciortino, Proc. Natl. Acad. Sci. U. S. A. **114**, 13336 (2017).
[35]P.-L. Chau and A. J. Hardwick, Mol. Phys. **93**, 511 (1998).
[36]P. J. Steinhardt, D. R. Nelson, and M. Ronchetti, Phys. Rev. B **28**, 784 (1983).
[37]T. M. Truskett, S. Torquato, and P. G. Debenedetti, Phys. Rev. E **62**, 993 (2000).
[38]W. Lechner and C. Dellago, J. Chem. Phys. **129**, 114707 (2008).
[39]F. Martelli, H.-Y. Ko, E. C. Oğuz, and R. Car, Phys. Rev. B **97**, 064105 (2018).
[40]J. R. Errington and P. G. Debenedetti, Nature **409**, 318 (2001).
[41]N. Giovambattista, P. G. Debenedetti, F. Sciortino, and H. E. Stanley, Phys. Rev. E **71**, 061505 (2005).
[42]J. Russo and H. Tanaka, Nat. Commun. **5**, 3556 (2014).
[43]A. Q. Tool, J. Am. Ceram. Soc. **29**, 240 (1946).
[44]R. Gardon and O. S. Narayanaswamy, J. Am. Ceram. Soc. **53**, 380 (1970).
[45]O. S. Narayanaswamy, J. Amer. Ceram. Soc. **54**, 491 (1971).
[46]C. T. Moynihan *et al.*, Ann. N. Y. Acad. Sci. **279**, 15 (1976).
[47]I. M. Hodge, J. Non-Cryst. Solids **169**, 211 (1994).
[48]I. M. Hodge and A. R. Berens, Macromolecules **15**, 762 (1981).
[49]A. J. Kovacs, J. J. Aklonis, J. M. Hutchinson, and A. R. Ramos, J. Polym. Sci., Polym. Phys. Ed. **17**, 1097 (1979).
[50]G. W. Scherer, *Relaxation in Glass and Composites* (Wiley, New York, 1986).
[51]N. Giovambattista, C. A. Angell, F. Sciortino, and H. E. Stanley, Phys. Rev. E **72**, 011203 (2005).
[52]J. P. Dyre, J. Chem. Phys. **143**, 114507 (2015).
[53]N. Giovambattista, H. E. Stanley, and F. Sciortino, Phys. Rev. E **69**, 050201(R) (2004).
[54]G. Sun, L. Xu, and N. Giovambattista, Phys. Rev. Lett. **120**, 035701 (2018).
[55]S. Mossa and F. Sciortino, Phys. Rev. Lett. **92**, 045504 (2004).
[56]R. L. Jack, L. O. Hedges, J. P. Garrahan, and D. Chandler, Phys. Rev. Lett. **107**, 275702 (2011).
[57]F. H. Stillinger and A. Rahman, J. Chem. Phys. **60**, 1545 (1974).
[58]M. P. Allen and D. J. Tildesley, *Computer Simulation of Liquids* (Oxford University Press, UK, 2002).
[59]P. H. Poole, I. Saika-Voivod, and F. Sciortino, J. Phys.: Condens. Matter **17**, L431 (2005).
[60]S. M. J. Rogge, L. Vanduyfhuys, A. Ghysels, M. Waroquier, T. Verstraelen, G. Maurin, and V. Van Speybroeck, J. Comput. Theory Comput. **11**, 5583 (2015).
[61]N. Giovambattista, F. W. Starr, and P. H. Poole, J. Chem. Phys. **147**, 044501 (2017).
[62]W. H. Press, B. P. Flannery, A. A. Teukolsky *et al.*, *Numerical Recipes: The Art of Scientific Computing* (Cambridge University, Cambridge, 1986).
[63]K. Winkel, R. Böhmer, F. Fujara, C. Gainaru, B. Geil, and T. Loerting, Rev. Mod. Phys. **88**, 011002 (2016).
[64]K. Winkel, D. T. Bowron, T. Loerting, E. Mayer, and J. L. Finney, J. Chem. Phys. **130**, 204502 (2009).
[65]P. H. Poole, S. R. Becker, F. Sciortino, and F. W. Starr, J. Phys. Chem. B **115**, 14176 (2011).